ISSN (Print) : 2320 – 3765
ISSN (Online): 2278 – 8875

International Journal of Advanced Research in Electrical, Electronics and Instrumentation Engineering

(An ISO 3297: 2007 Certified Organization)

Vol. 3, Issue 11, November 2014

High Efficiency Ac-Ac Power Electronic Converter Applied To Domestic Induction Heating

S.Prakash[1], Jafar Ali[2]

Associate Professor, Dept of EEE, Bharath University, Chennai, Chennai, Tamil Nadu, India[1]

Dept of EEE, Bharath University, Chennai, Tamil Nadu, India[2]

ABSTRACT: In the conventional, induction heating application, several resonant matrix converters featuring MOSFETs have been proposed. However, the final efficiency and cost are compromised due to the use of a higher number of switching devices. The proposed topology, based on the half-bridge series resonant inverter, uses only two diodes to rectify the mains voltage. The proposed converter can operate with zero-voltage switching during both switch-on and switch-off transitions.
The closed loop system is analyzed in this Paper by active filter control technique where a smooth sinusoidal wave is formed at the load side. The MOSFETs are operated by switching frequency of 50kHz. As a consequence, the converter efficiency is significantly improved. AC-AC converter is simulated using the software MATLAB and is implemented in a prototype model.

I. INTRODUCTION

AC-AC CONVERTERS

An ac voltage controller is a type of thyristor power converter which isused to convert a fixed voltage, fixed frequency ac input supply to obtain a variablevoltage ac output. [1-3]The RMS value of the ac output voltage and the ac power flow to the load is controlled by varying the trigger angle 'α'.
AC-AC converters can be categorized as follows:

- Indirect AC-AC (or AC-DC-AC) converters (i.e., with rectifier, DC link and inverter).
- Cycloconverter.
- Hybrid matrix converters.
- Matrix converters (MC).

An AC-AC converter with approximately sinusoidal input currents and bidirectional power flow can be realized by coupling a pulse width modulation (PWM) rectifier and a PWM inverter to the DC-link. The DC-link quantity is then impressed by an energy storage element that is common to both stages, which is a capacitor C for the voltage DC-link or an inductor L for the current DC-link.[4] The PWM rectifier is controlled in a way that a sinusoidal AC line current is drawn, which is in phase or anti-phase (for energy feedback) with the corresponding AC line phase voltage.

CYCLOCONVERTER

This converter converts single-phase or three-phase AC power to single-phase or three-phase power having a variable frequency and magnitude. Typically, the output frequency of the AC power is lower than the input frequency.[5] A cycloconverter has the capacity to operate with loads of variable power factors and also allows bidirectional power flow. They can be broadly classified into two types phase-controlled cycloconverters and envelope cycloconverters. In the former, control of the firing angle is accomplished through adjustable gate impulses, while in the latter, the switches remain in an on state and conduct in consecutive half cycles. [6-8]

ISSN (Print) : 2320 – 3765
ISSN (Online): 2278 – 8875

International Journal of Advanced Research in Electrical, Electronics and Instrumentation Engineering

(An ISO 3297: 2007 Certified Organization)

Vol. 3, Issue 11, November 2014

They are mostly used to control the speed of drives and for converting variable input frequency power into constant frequency output, such as in very high-power applications, including driving synchronous motors and induction motors. Some of the places where cycloconverters are employed include cement mill drives, mine winders, and ore grinding mills. They are also utilized in ship propulsion drives, scherbius drives, and rolling mill drives.[9]

Offering many advantages, a cycloconverter can be used in quite a few low-speed applications and is also a compact system. Its ability to directly affect the frequency conversion of power without any intermediate stage involving DC power is another huge advantage. If the cycloconverter experiences a commutation failure, the results are minimal, such as the blowing off of individual fuses. [10]

It also has the capacity of regeneration, covering the total range of speeds. Another huge advantage of the cycloconverter is its ability to deliver a sinusoidal waveform at a lower output frequency. This advantage comes from its ability synthesize the output waveform using a large number of segments of the input waveform.

This technology does have some disadvantages, though. Firstly, the frequency of the output power is around one third or less of the input frequency. It's possible to improve the quality of the output waveform if a larger number of switching devices are employed. A cycloconverter requires quite a complex control mechanism and also uses a large quantity of thyristors. Its use is also limited by severe harmonics and the low-output frequency range.

In the past, several ac–ac topologies have been proposed to simplify the converter and improve the efficiency. Considering the induction heating application, several resonant matrix converters featuring MOSFETs have been proposed. However, the final efficiency and cost are compromised due to the use of a higher number of switching devices. Other approaches, commonly used in electronic ballasts, simplify the rectifier stage in order to improve the converter performance. This topology, known as half-bridge boost rectifier, reduces the switch count while keeping the same performance as more complex solutions.

In this Paper,the principle of operation is based on the generation of a variable magnetic field by means of a planar inductor below a metallic vessel. The mains voltage is rectified and after that an inverter provides a medium-frequency current to feed the inductor. The usual operating frequency is higher than 20 kHz to avoid the audible range and lower than 100 kHz to reduce switching losses. [11]

The most used device is the insulated gate bipolar transistor (IGBT) because of the operating frequency range and the output power range, up to 3 kW. Nowadays, most designs use the half-bridge series resonant topology because of its control simplicity and high efficiency.

The scope of the Paper is to design a resonant converter in direct AC-AC conversion and its efficiency while reducing the power device count for induction heating applications.[12-15] The proposed topology is based on the series resonant half-bridge topology and requires only two rectifier diodes. Moreover,it can operate with zero-voltage switching conditions during turn-on for both switching devices, and also during turn-off transitions for one of them. As a consequence, the efficiency is improved while the device count is reduced.

II. HIGH EFFICIENCY AC-AC POWER ELECTRONIC CONVERTER APPLIED TO DOMESTIC INDUCTION HEATING

The proposed topology shown in **Fig.2.1** employs two bidirectional switches $S_H$and $S_L$composed of a transistor $T_H$or T_L, typically an IGBT, and an anti-parallel diode $D_H$or D_L respectively. The mains voltage $V_{ac}$is rectified by two diodes $D_{rH}$and D_{rL}, but only one of them is activated at the same time. This operation increases efficiency with regard to classical topologies based on a full-bridge diode rectifier plus a dc-link inverter.

ISSN (Print) : 2320 – 3765
ISSN (Online): 2278 – 8875

International Journal of Advanced Research in Electrical, Electronics and Instrumentation Engineering

(An ISO 3297: 2007 Certified Organization)

Vol. 3, Issue 11, November 2014

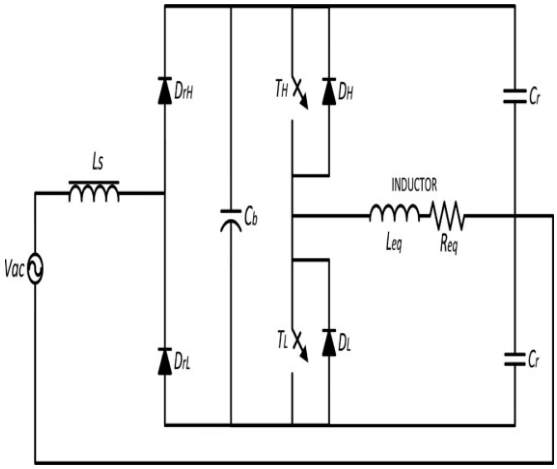

Fig.2.1. Proposed Converter Circuit

The proposed topology is a series–parallel resonant converter. The inductor–pot system is modeled as an equivalent series resistance $R_{eq}$and inductance L_{eq}, as shown in **Fig.2.1**. This topology implements resonant capacitors $C_r$and may use a bus capacitor C_b. Due to the symmetry between positive and negative mains voltage, both resonant capacitors have the same value. An input inductor $L_s$is used to reduce the harmonic content to fulfill the electromagnetic compatibility regulations.[16]

ANALYSIS

The topology presents symmetry between positive and negative ac voltage supply. Its symmetry simplifies analysis and makes possible to redraw the circuit as shown in **Fig.2.2.** Although this topology uses different resonant configurations, parallel and series, and different resonant tanks for each of them, it is possible to use a normalized nomenclature based on series resonance

$C_b = \alpha . C_r \quad \alpha \geq 0$
$L_S = \beta . L_{eq} \quad \beta \geq 1$
$\omega_0 = 1/(L_{eq}.C_r)^{1/2}$
$\omega_n = \omega_{sw}/\omega_o$
$Z_O = (L_{eq}/C_r)^{1/2}$

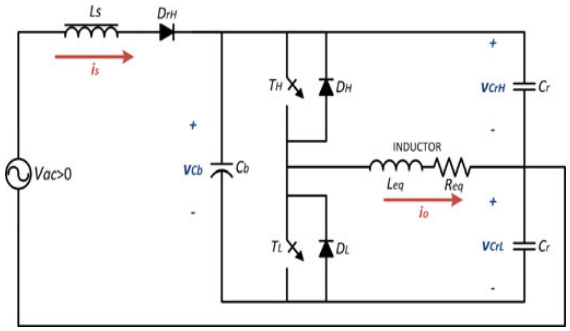

Fig.2.2. Equivalent circuit during the positive mains voltage cycle

Where α is the ratio between the dc-link and the resonant capacitors and β is the ratio between the input choke and the equivalent inductance of the inductor–pot system. The parameters $\{\omega_0, \omega_{sw}, \omega_n\}$are the angular resonant frequency, the angular switching frequency, and the normalized angular switching frequency, respectively. Z_0defines the equivalent impedance of the resonant circuit, defined by $L_{eq}$and C_r. Finally, $Q_{eq}$is the equivalent inductor–pot system quality factor

10.15662/ijareeie.2014.0311173

ISSN (Print) : 2320 – 3765
ISSN (Online): 2278 – 8875

International Journal of Advanced Research in Electrical, Electronics and Instrumentation Engineering

(An ISO 3297: 2007 Certified Organization)

Vol. 3, Issue 11, November 2014

at the resonant frequency. The system will be analyzed using the state-space description. Each state is completely defined by a differential equation system and the global system response is the conduction angle, θ, average response of each state (I–III).As is shown in **Fig.2.3-2.5**, working under ZVS conditions, there are three different states.

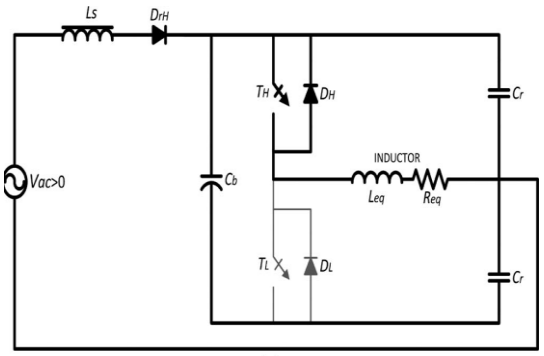

Fig.2.3. Equivalent Circuit : State I

State I operates with the high-side switching device $S_H$triggered-on and activated and the low-side switching device (S_L) triggered-off. The parallel resonant circuit is set by an equivalent capacitor C_{eq}, obtained from $C_r$and $C_b$and expressed below, and the inductor electrical parameters, $R_{eq}$and L_{eq}. The current flowing through $S_H$is the same as the one flowing through the load.

State I begins when $S_L$is triggered OFF. In this moment, the anti-parallel diode $D_H$conducts and $S_H$can be triggered ON ensuring ZVS switching-on conditions. Transitions from this state can lead either to state II or state III. If voltage across $S_L$reaches zero and $D_L$starts conducting, the transition condition to state II is fulfilled. On the other hand, if $S_H$is switched OFF when T_H conducts, the next state is state III.

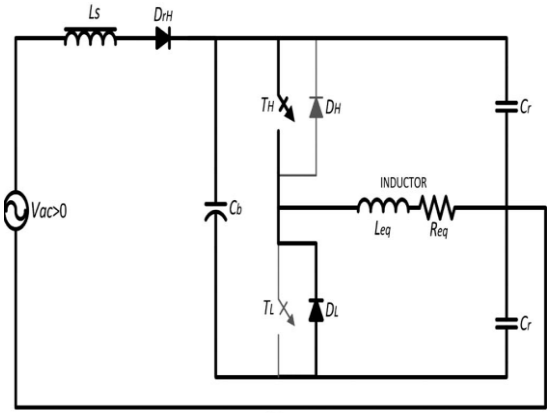

Fig.2.4. Equivalent Circuit : State II

State II is characterized by the conduction of both switching devices, although only $S_H$is triggered ON. That is, $T_H$and $D_L$conduct at the same time. Current through load is supplied by both devices ($T_H$and D_L), and consequently, low conduction stress for the devices is achieved. The equivalent parallel resonant circuit is set by the inductor electrical parameters in parallel with both resonant capacitors. $C_b$is short-circuited by both switching devices. This state starts when the voltage across $S_L$reaches zero. At this moment, $D_L$starts conducting at the same time as $T_H$is triggered ON. This state finishes when $S_H$is triggered OFF and the next state is state III. The main benefit results of the lower switch-off current achieved when $S_H$is triggered OFF, due to the fact that the load current is supplied by both devices.

ISSN (Print) : 2320 – 3765
ISSN (Online): 2278 – 8875

International Journal of Advanced Research in Electrical, Electronics and Instrumentation Engineering

(An ISO 3297: 2007 Certified Organization)

Vol. 3, Issue 11, November 2014

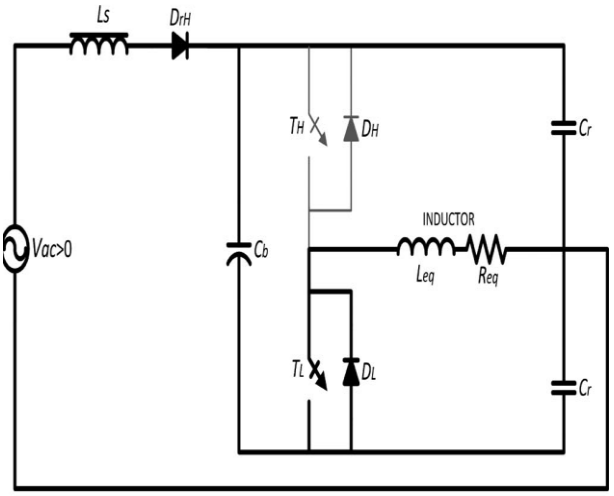

Fig.2.5. Equivalent Circuit: State III

State III is defined by the conduction of $S_L$while $S_H$is deactivated. The equivalent resonant circuit is set by one resonant capacitor in parallel with the series connection of the $C_b$capacitor and the parallel connection of the inductor and the other one resonant capacitance. Note that when $C_b$is zero ($\alpha = 0$), the equivalent resonant circuit is a series RLC circuit composed of the inductor–pot system and one resonant capacitor. This state starts when $S_H$is triggered OFF. At this moment, $D_L$starts conducting and $S_L$can be triggered ON achieving ZVS switch-on conditions. This state finishes when $S_L$is deactivated, and the next state is state I.

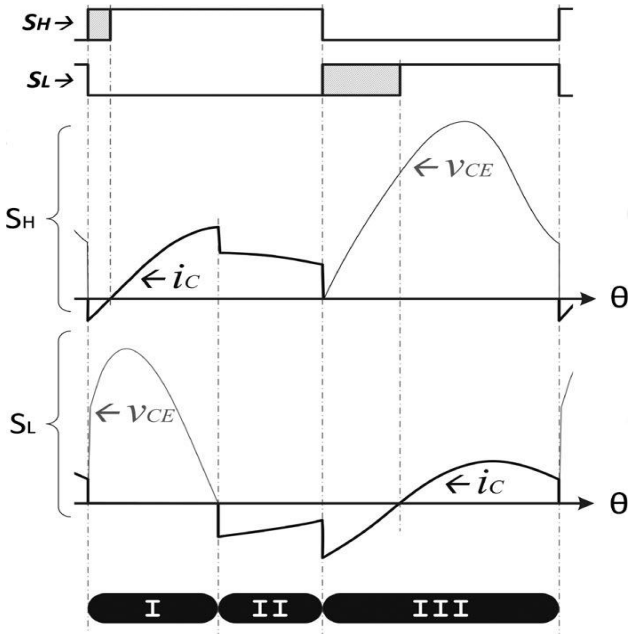

Fig.2.6. Switching Pattern of the two switches

ISSN (Print) : 2320 – 3765
ISSN (Online): 2278 – 8875

International Journal of Advanced Research in Electrical, Electronics and Instrumentation Engineering

(An ISO 3297: 2007 Certified Organization)

Vol. 3, Issue 11, November 2014

Asymmetrical Duty Cycle Control

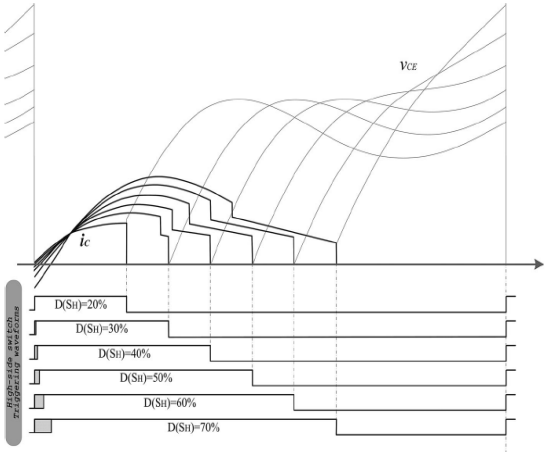

Fig.2.7. ADC control strategy: main control signals and waveforms.

The ADC control varies the output power by changing the switching device duty cycle. As is shown in **Fig.2.7**, this control strategy delivers different output powers by changing the percent of conducting angle (θ) in which the high-side switch $S_H$is activated D_{SH}. The low-side switch $S_L$conducting angle can be calculated as follows:

$$D(S_L)=2\pi-D(S_H)-\theta_{DT}$$

where$\theta_{DT}$is the dead-time conducting angle to avoid short circuits. The variation of conducting angle is restricted by the achievement of soft-switching conditions for S_H, ZVS for switching-off, and by the achievement of ZVS in the switching on commutation for both devices (anti-parallel diode conduction at the beginning). In order to operate with switch-on ZVS conditions, the duty cycle must be higher than 30%. The upper boundary is kept to 60% to obtain a proper safety margin and balance the total amount of losses per switching device.

III. SIMULATION RESULTS

MATLAB (**mat**rix **lab**oratory) is a numerical computing environment and fourth-generation programming language.Developed by Mathworks. MATLAB allows matrix manipulations, plotting of functions and data, implementation of algorithms, creation of user interfaces, and interfacing with programs written in other languages, including C, C++, Java, and Fortran.

Simulink is a block diagram environment for multi-domain simulation and Model-Based Design. Simulink provides a graphical editor, customizable block libraries, and solvers for modeling and simulating dynamic systems.

STEPS FOR DOING SIMULATION IN MATLAB

STEP 1:Building the Model

STEP 2:Simulating the Model

STEP 3:Running the Simulation

STEP 4:Analyzing Simulation Results

STEP 5:Viewing Simulation Results

STEP 6:Debugging the Simulation

ISSN (Print) : 2320 – 3765
ISSN (Online): 2278 – 8875

International Journal of Advanced Research in Electrical, Electronics and Instrumentation Engineering

(An ISO 3297: 2007 Certified Organization)

Vol. 3, Issue 11, November 2014

OPEN LOOP SYSTEM

The open loop system is implemented in MATLAB SIMULINK. As per the converter pulse design, a simulation is performed based on the switching explained in the second chapter.

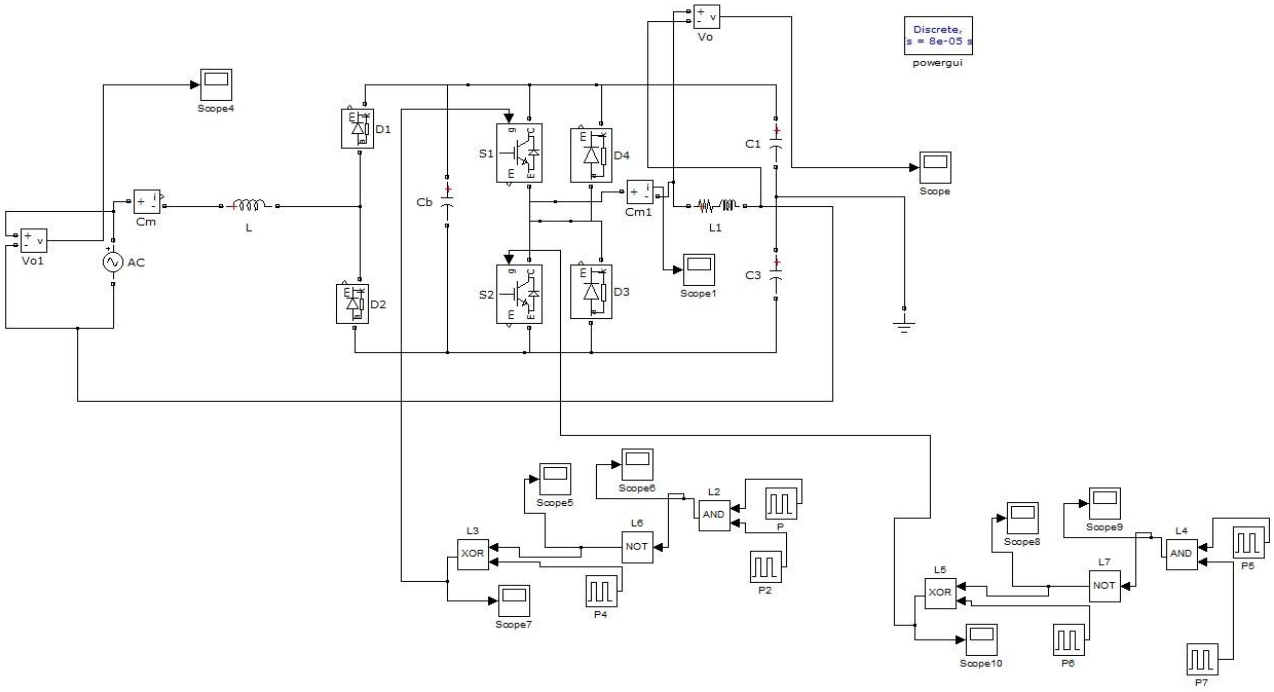

Fig.3.1. Simulation of the open loop system of the converter in MATLAB

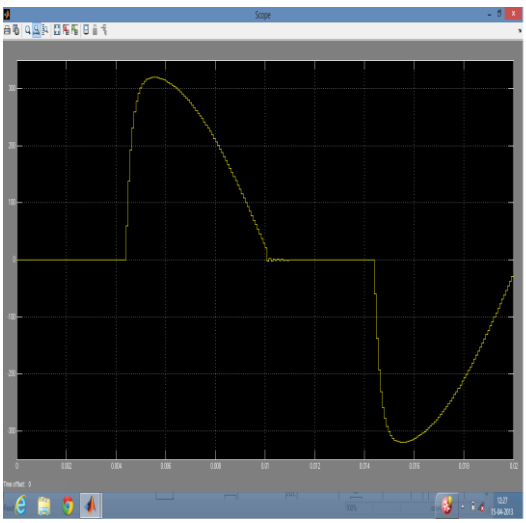

Fig.3.2.Open Loop Output Voltage Waveform

ISSN (Print) : 2320 – 3765
ISSN (Online): 2278 – 8875

International Journal of Advanced Research in Electrical, Electronics and Instrumentation Engineering

(An ISO 3297: 2007 Certified Organization)

Vol. 3, Issue 11, November 2014

X-axis:Time in secs
Y-axis:Amplitude in volt

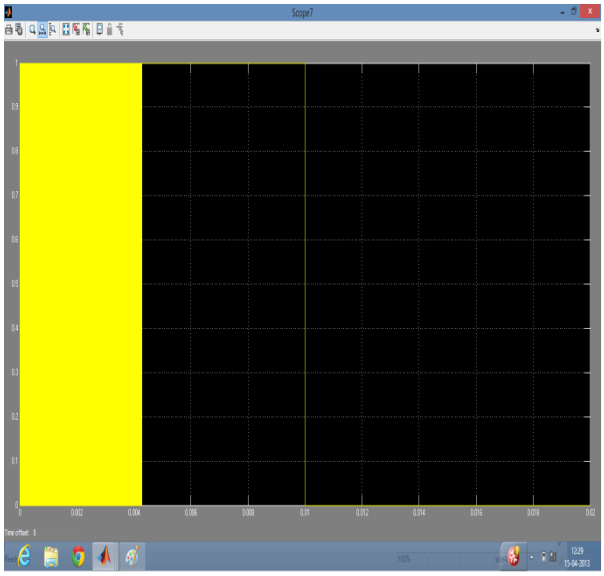

Fig.3.3.Switching of S_H

The above figure depicts the triggering pulses to high side switching device
X-axis:Time in secs
Y-axis:Amplitude in volt

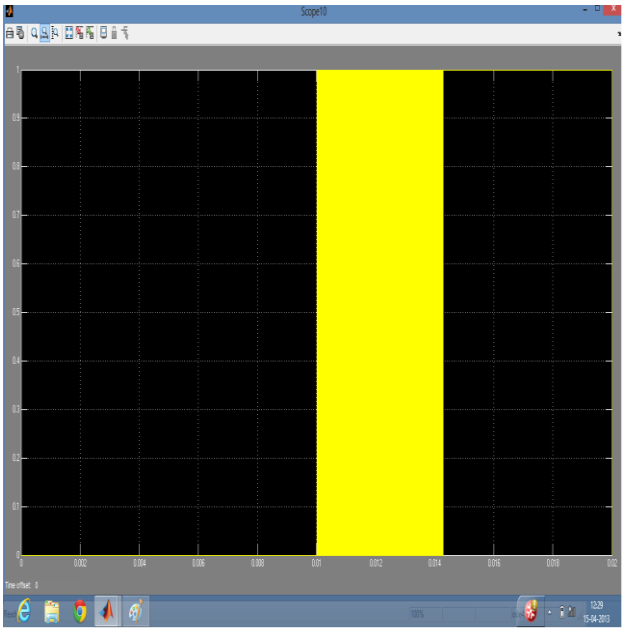

Fig.3.4.Switching of S_L

ISSN (Print) : 2320 – 3765
ISSN (Online): 2278 – 8875

International Journal of Advanced Research in Electrical, Electronics and Instrumentation Engineering

(An ISO 3297: 2007 Certified Organization)

Vol. 3, Issue 11, November 2014

The above figure depicts the triggering pulses of low side switching device.
X-axis:Time in secs.
Y-axis:Amplitude in volt.

CLOSED LOOP SYSTEM

The closed loop system is implemented in MATLAB SIMULINK. For closed loop simulation using PI controller, the proposed resonant converter is considered. Simulated results are presented.

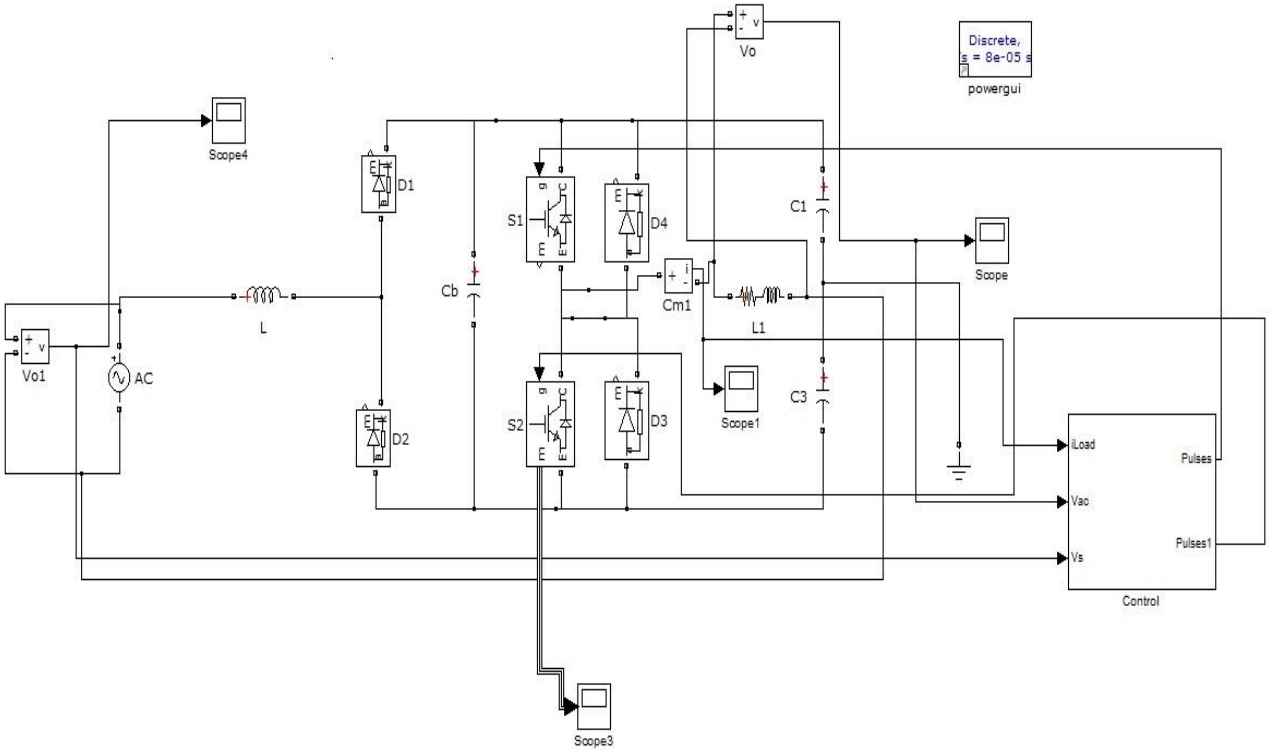

Fig.3.5. Simulation of the closed loop system of the converter in MATLAB

ISSN (Print) : 2320 – 3765
ISSN (Online): 2278 – 8875

International Journal of Advanced Research in Electrical, Electronics and Instrumentation Engineering

(An ISO 3297: 2007 Certified Organization)

Vol. 3, Issue 11, November 2014

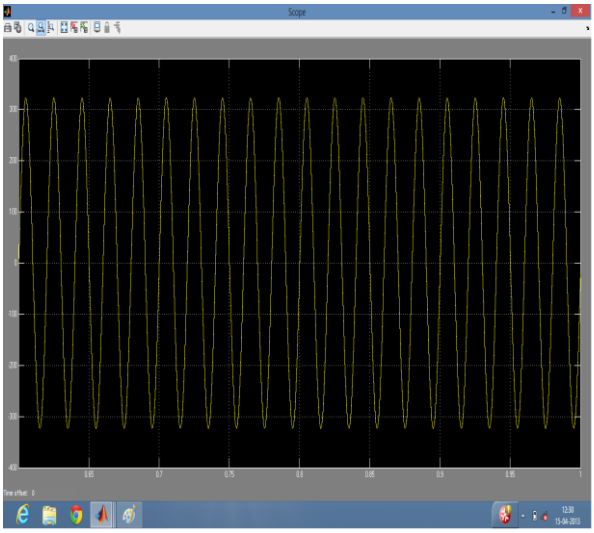

Fig.3.6.Closed Loop Output Voltage Waveform

The above figure depicts the closed loop output voltage waveform.

X-axis:Time in secs
Y-axis:Amplitude in volt

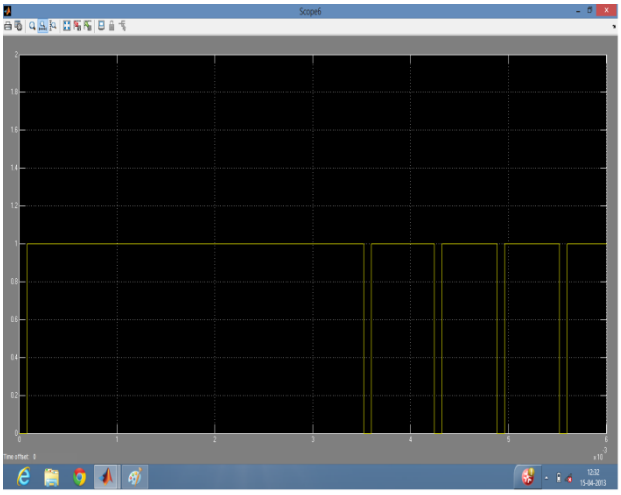

Fig.3.7. Switching of S_H

The above figure depicts the triggering pulses to $S_{H.}$

X-axis:Time in sec.
Y-axis:Amplitude in volt

ISSN (Print) : 2320 – 3765
ISSN (Online): 2278 – 8875

International Journal of Advanced Research in Electrical, Electronics and Instrumentation Engineering

(An ISO 3297: 2007 Certified Organization)

Vol. 3, Issue 11, November 2014

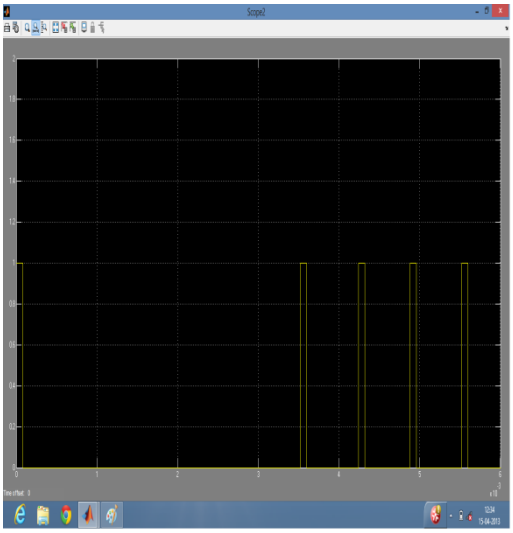

Fig.3.8 Switching of S_L

The above figure depicts the triggering pulses to $S_{L.}$
X-axis:Time in sec.
Y-axis:Amplitude in volt

CLOSED LOOP DESIGN

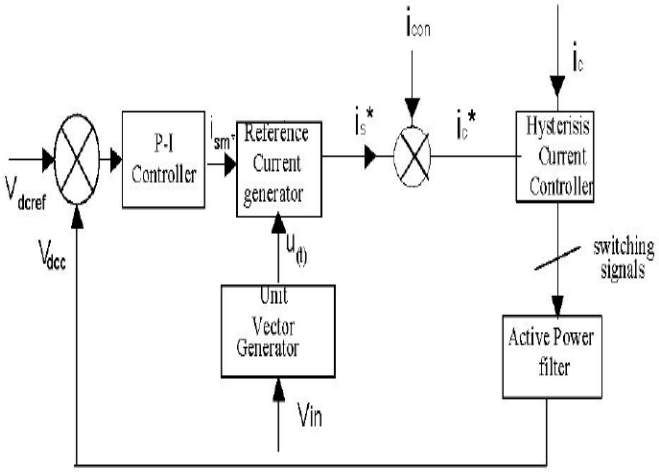

Fig. 3.9. Closed loop system implemented in SIMULINK

The main section of the converter shown in the chapter 2 is connected to the dc bus capacitor. The current harmonic compensation is achieved by injecting the equal but opposite current harmonic at the point of connection, thereby canceling the original distortion and improving the power quality on connected power system. Instantaneous dc bus voltage (V_{dc}), supply voltage (V_i) and converter current (icon) are sensed to obtain the switching signals to control the switching devices of converter. The ac source supplies the fundamental active power component of the converter current and the fundamental component of current to maintain average dc bus voltage of the converter to a constant value. The later component of current is to supply losses in converter, such as switching losses, capacitor leakage current etc. The sensed dc bus voltage (V_{dc}) is compared with the dc reference voltage (V_{dcref}). The output of the

10.15662/ijareeie.2014.0311173

ISSN (Print) : 2320 – 3765
ISSN (Online): 2278 – 8875

International Journal of Advanced Research in Electrical, Electronics and Instrumentation Engineering

(An ISO 3297: 2007 Certified Organization)

Vol. 3, Issue 11, November 2014

comparator is error signal $e_r(t)$. This error signal is then processed in a P-I controller and the peak value of reference supply current (I_{sm}) is obtained. The unit vector $u_r(t)$ of supply voltage is derived from its sensed value. The peak value of reference supply current (I_{sm}) is multiplied with the unit vector to generate reference sinusoidal unity power factor current. The reference supply current (i_r*) is compared with the actual converter current (icon) to give reference converter current (i_r*). The actual converter current (i_j) and the reference converter current (i_c*) are processed in a hysteresis current controller to derive gating signals of the devices (MOSFETs) of the converter. The corrective action is taken in each half cycle of the ac source, resulting in fast dynamic response of the converter. The output voltage of the converter is regulated by varying the switching frequency or by controlling the duty ratio.[17]In the open loop system design in SIMULINK, the simulation of this resonant converter is presented where the AC voltage of 325V (V_{peak}) is converted in to 325Vac directly. The effect of the output voltage is presented with graphs above.

In the closed loop system design in SIMULINK, the simulation of 325V (V_{peak}) is converted in to 325V using PI controllers for the values of k_p=1; k_i=1. The input voltage is multiplied by 1/$V_{peak}$and the resultant signal is subtracted with the input current for unity power factor operation, then the signal is compared with the load current. Then the pulses is driven to switches S_1&S_2. The effect of sinusoidality is pure by the closed loop system.

IV. HARDWARE DESCRIPTION

HARDWARE REQUIREMENTS

Power MOSFET	:	IRF840
Driver IC	:	IR2112
Capacitor	:	470uF (25V); 1000uF; 4700uF
Inductor	:	100uH; 200uH
Controller	:	PIC16F877A
Regulators	:	LM7805; LM7812
Diodes	:	1N4000; 1N5407; 1N5408

CIRCUIT DIAGRAM

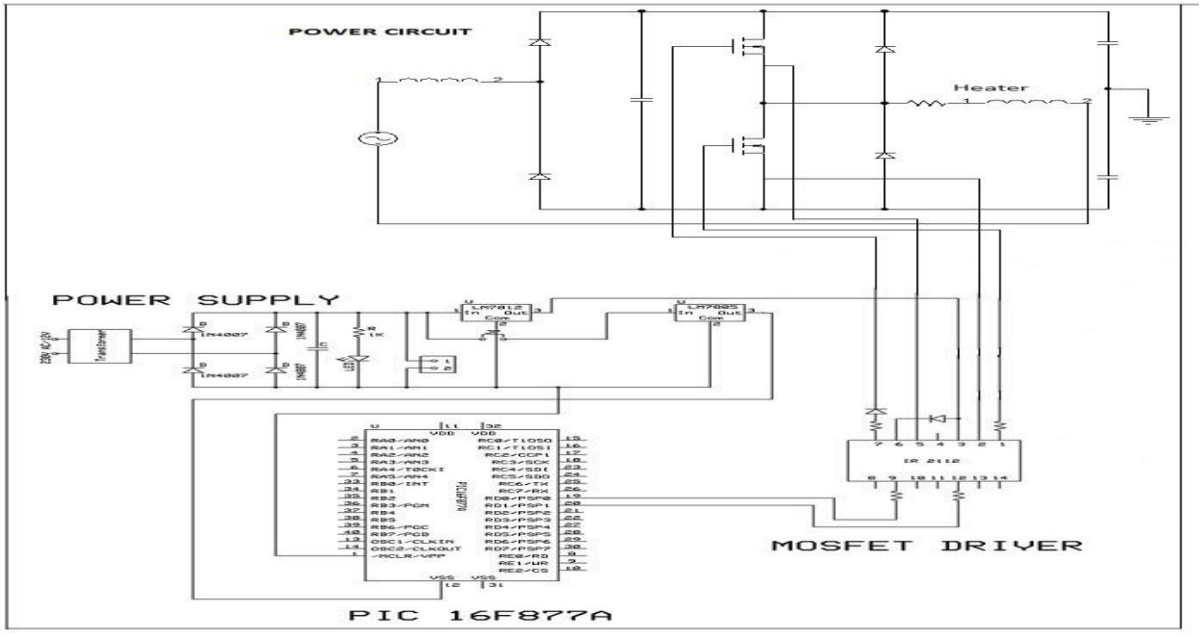

Fig.4.2.Circuit Diagram

ISSN (Print) : 2320 – 3765
ISSN (Online): 2278 – 8875

International Journal of Advanced Research in Electrical, Electronics and Instrumentation Engineering

(An ISO 3297: 2007 Certified Organization)

Vol. 3, Issue 11, November 2014

EXPECTED INPUT AND OUTPUT

- **Given Input:**
  The 230Vac from the input side is fed to the power circuit.
- **Expected Output:**
  By using the controller circuit and driver circuit, and then switching the converter, the 230Vac is got as output at the load side from the 230Vac.

PROTOTYPE PARAMETERS

The following table gives the values of parameters used for prototype.

Table 5.1. Prototype Parameters

	COMPONENTS	VALUES
L_{eq}	EQUIVALENT INDUCTANCE	65µH
R_{eq}	EQUIVALENT RESISTANCE	6.5Ω
V_{ac}	POWER SUPPLY	325V
C_r	RESONANT CAPACITOR	470nF
C_b	DC-LINK CAPACITOR	0nF
L_a	INPUT IMPEDANCE	1.4mH
S_H, S_L	SWITCHING DEVICE WITH ANTIPARALLEL DIODE	IGBTFGH30RN120
D_{rH}, D_{rL}	RECTIFIER DIODES	DESP 6012AR

HARDWARE RESULTS

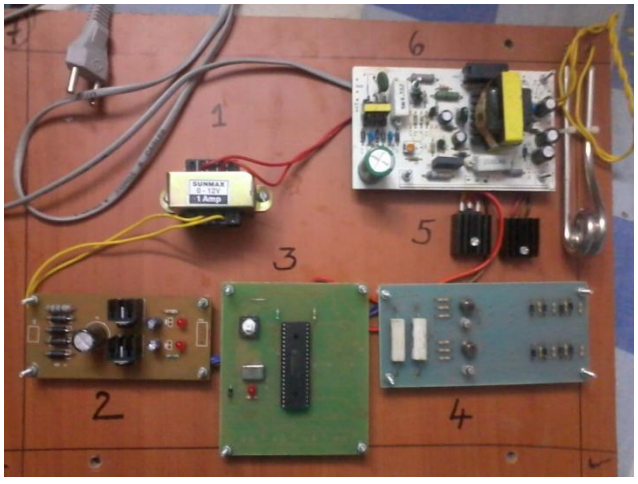

HARDWARE KIT

V. CONCLUSION

In this Paper, a new ac–ac converter applied to domestic induction heating. An analytical analysis has been performed in order to obtain the equations and operation modes that describe the proposed converter. The converter can operate with zero-voltage switching during both turn-on and turn-off commutations. As a consequence, the power converter efficiency is improved in the whole operating range. The design is implemented in MATLAB SIMULINK and the

ISSN (Print) : 2320 – 3765
ISSN (Online): 2278 – 8875

International Journal of Advanced Research in Electrical, Electronics and Instrumentation Engineering

(An ISO 3297: 2007 Certified Organization)

Vol. 3, Issue 11, November 2014

results are presented. The hardware is implemented in a prototype model using PIC microcontroller and the results are presented.

FUTURE ENHANCEMENT

In this Paper, the proposed converter is useful for future applications. This converter can be further improved by using motors instead of load and using FPGA instead of microcontroller unit.

REFERENCES

1. Advanced Micro Devices, A.M.D., 1996. Magic packet technology application in hardware and software. Publication, 20381.
2. Subha Palaneeswari M., Abraham Sam Rajan P.M., Silambanan S., Jothimalar, "Blood lead in end-stage renal disease (ESRD) patients who were on maintainence haemodialysis", Journal of Clinical and Diagnostic Research, ISSN : 0973 - 709X, 6(10) (2012) pp.1633-1635.
3. Sharmila S., Rebecca L.J., Saduzzaman M., "Effect of plant extracts on the treatment of paint industry effluent", International Journal of Pharma and Bio Sciences, ISSN : 0975-6299, 4(3) (2013) pp.B678-B686.
4. Electronic Products Company, EPC, 1996. Trickle Power: Power management of integrated circuits at the microchip level. Application Note PM-403.
5. Herring, H., 1996. Standby power consumption in brown goods, A case study of hi-fi equipment. Open University EERU Report No. 73, September. Milton Keynes, England.
6. Jeyanthi Rebecca L., Dhanalakshmi V., Sharmila S., "Effect of the extract of Ulva sp on pathogenic microorganisms", Journal of Chemical and Pharmaceutical Research, ISSN : 0975 – 7384 , 4(11) (2012) pp.4875-4878.
7. Sharmila D., Saravanan S., "Efficacy of lead on germination growth and morphological studies of Horse Gram (Dolichos biflorus Linn)", Journal of Chemical and Pharmaceutical Research, ISSN : 0975 – 7384 , 4(11) (2012) pp.4894-4896.
8. Prakash. S, "Digital Simulation of B.L.D.C Motor Drive System with Energy Recovery Snubber" World Applied Sciences Journal, ISSN 1818-4952, pp 1107 – 1116, 2014.
9. Prakash. S, "Energy Conservation through Stanby Power Reduction" Middle east Journal of Scientific Research 19(7) , ISSN 1900-9233, pp 990 – 994, 2014.
10. Prakash. S, "Advanced Controller Design for PMBLDC Motor – A review" Middle east Journal of Scientific Research 19(8) , ISSN 1900-9233, pp 1041-1046, 2014.
11. Prakash. S, "Modern Measures to Reduce the Impact of Lightning" Middle east Journal of Scientific Research 19(8) , ISSN 1900-9233, pp 919-927, 2014.
12. Prakash. S, "Design and Analysis of Resonant Soft Switching Chopper" Middle east Journal of Scientific Research 19(8) , ISSN 1900-9233, pp 913-918, 2014.
13. Byoung-KukLee, Member; IEEE, Tae-Hyung Kim, Student Member; IEEE, and Mehrdad Ehsani, Fellow, IEEE, "On the Feasibility of Four-Switch Three Phase BLDC Motor Drives for Low Cost Commercial Applications: Topology and Control" IEEE Transactions on Power Electronics, Vol, 18.No.1, January 2003.
14. Saduzaman M., Sharmila S., Jeyanthi Rebecca L., 'Efficacy of leaf extract of Moringa oleifera in treating domestic effluent", Journal of Chemical and Pharmaceutical Research, ISSN : 0975 – 7384, 5(2) (2013) pp.139-143.
15. R.Krishnan, Senior Member, IEEE and Shiyoung Lee "PM Brushless DC Motor Drive with a New Power-Converter Topology", IEEE Transactions on Industry applications, Vol.33.No.4,July/August 1997.
16. Rahul Khopkar, S.M.Madani, Masoud Hajiaghajani, Hamid A.Toliyat "A Low Cost BLDC Motor Drive using Buck-Boost Converter for residential and commercial Applications" IEEE Int. Conf. on Electric Machines and Drives' IEMDC'03, Vol-2,pp-1251-1257, Jun2003.
17. F.L.Luo, and H.Ye "Energy Factor and Mathematical modeling for power dc-dc converters", Proc Inst.Elect.Eng, Vol 152, No 2 pp. 191-198, Mar.2005.
18. Premkumar, S., Ramu, G., Gunasekaran, S., Baskar, D., "Solar industrial process heating associated with thermal energy storage for feed water heating", Middle - East Journal of Scientific Research, v-20, i-11, pp:1686-1688, 2014.
19. Premkumar, S., Prabhakar, S., Lingeswaran, K., Ramnathan, P., "Development of direct methanol fuel cell and improving the efficiency", Middle - East Journal of Scientific Research, v-20, i-10, pp:1277-1280, 2014.
20. B.Vamsi Krishna, Significance of TSC on Reactive power Compensation, International Journal of Advanced Research in Electrical, Electronics and Instrumentation Engineering, ISSN (Online): 2278 – 8875,pp 7067-7078, Vol. 3, Issue 2, Febuary 2014
21. Mr D.Sridhar raja,Wireless Transmission of Real Time Electrocardiogram (ECG) Signals through Radio Frequency (RF) Waves,International Journal of P2P Network Trends and Technology(IJPTT),ISSN: 2278 – 8875 , pp 793-798, Vol. 2, Issue 2, February 2013.
22. E.Kanniga, N. Imocha Singh ,K.Selva Rama Rathnam ,Gated-Demultiplexer Tree Buffer for Low Power Using Clock Tree Based Gated Driver, International Journal of P2P Network Trends and Technology(IJPTT), ISSN (Print) : 2320 – 3765, pp 4652-4659 ,Vol. 2, Issue 10, October 2013